

Article

## Characterization of Laser Beam Shaping Optics Based on Their Ablation Geometry of Thin Films

Stefan Rung \*, Johannes Barth and Ralf Hellmann

University of Applied Science Aschaffenburg, Wuerzburger Strasse 45, D-63743 Aschaffenburg, Germany; E-Mails: s8443@h-ab.de (J.B.); ralf.hellmann@h-ab.de (R.H.)

\* Author to whom correspondence should be addressed; E-Mail: stefan.rung@h-ab.de; Tel.: +49-602-1420-6928; Fax: +49-602-1420-6801.

External Editors: Maria Farsari and Costas Fotakis

Received: 9 September 2014; in revised form: 20 October 2014 / Accepted: 21 October 2014 / Published: 27 October 2014

---

**Abstract:** Thin film ablation with pulsed nanosecond lasers can benefit from the use of beam shaping optics to transform the Gaussian beam profile with a circular footprint into a Top-Hat beam profile with a rectangular footprint. In general, the quality of the transformed beam profile depends strongly on the beam alignment of the entire laser system. In particular, the adjustment of the beam shaping element is of utmost importance. For an appropriate alignment of the beam shaper, it is generally necessary to observe the intensity distribution near the focal position of the applied focusing optics. Systems with a low numerical aperture (NA) can commonly be qualified by means of laser beam profilers, such as a charge-coupled device (CCD) camera. However, laser systems for micromachining typically employ focus lenses with a high NA, which generate focal spot sizes of only several microns in diameter. This turns out to be a challenge for common beam profiling measurement systems and complicates the adjustment of the beam shaper strongly. In this contribution, we evaluate the quality of a Top-Hat beam profiling element and its alignment in the working area based on the ablated geometry of single pulse ablation of thin transparent conductive oxides. To determine the best achievable adjustment, we develop a quality index for rectangular laser ablation spots and investigate the influences of different alignment parameters, which can affect the intensity distribution of a Top-Hat laser beam profile.

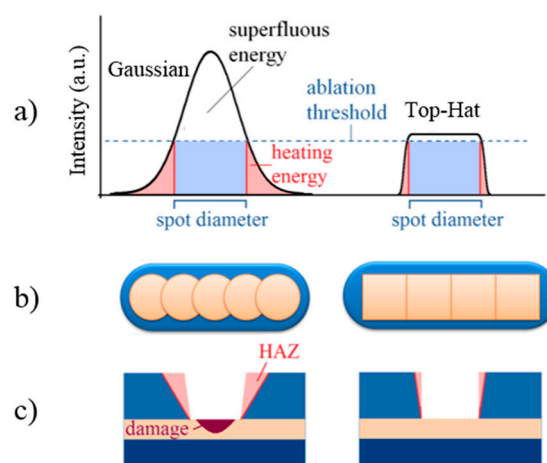
**Keywords:** laser beam shaping; diffractive optical element (DOE); Top-Hat; transparent conductive oxides (TCO); indium tin oxide (ITO); thin film; laser ablation

---

## 1. Introduction

For thin film ablation with pulsed nanosecond lasers, the advantages of a spatially-optimized laser beam profile have been demonstrated in many studies [1–5]. In comparison to the common Gaussian beam profile with a circular footprint of Q-switched diode pumped solid state lasers (DPSSL), the use of a Top-Hat laser beam profile with a rectangular footprint provides several benefits for laser ablation of thin films (*cf.* Figure 1). For instance, the homogenous part of the laser beam profile can be tuned in intensity close to the ablation threshold. Thereby, the excess energy not contributing to the ablation process is small, and consequently, less energy enters the underlying substrate, where it can negatively affect the substrate properties [6]. Secondly, the Top-Hat laser beam profile possesses steeper wings than the Gaussian energy distribution. As a result, the material adjacent to the ablation region has to absorb less energy, which, in turn, reduces the undesired modifications of the remaining thin film properties [6]. Besides these benefits resulting from the intensity plateau and the steep wings of the intensity distribution, the transformation of a round laser footprint into a rectangular footprint can additionally improve the scribing process significantly, as illustrated in Figure 1b [7]. Whereas a pulsed laser with a round laser footprint generates a saw tooth pattern along the rim of an ablated line, a rectangular laser footprint circumvents such a pattern. Moreover, the pulse overlap can be reduced for a high quality ablation pattern with straight laser scribed lines [8]. However, contrary to the idealized representation of the laser scribed line consisting of a series of perfectly rectangular-shaped laser footprints shown in Figure 1b, the ablation spot of a single laser pulse will display deviations from the rectangular geometry, such as, e.g., rounding at the corners.

**Figure 1.** Different ablation behavior of thin films for Gaussian (**left**) and Top-Hat (**right**) laser beam profiles. **(a)** Cross-section of laser beam profiles; **(b)** ablated line with circular and rectangular laser footprint; **(c)** cross section of the processed material system with implied heat affected zone (HAZ) [4].



For laser micromachining application, often, diffractive Top-Hat beam shaping optics are employed [1,2,6,7]. The resulting laser beam profile of such diffractive beam shapers depends strongly on, e.g., the position of the working plane, the free aperture of the beam delivery path and, certainly, on the adjustment of the beam shaper itself. Opposite of a Gaussian beam profile, the energy distribution of a diffractively-shaped laser beam changes along the propagation direction after a convex lens, which is

used for focusing the beam onto the processed work piece. Consequently, it is necessary to observe the beam profile in the focal spot to give information about the beam shaping result. With commonly used imaging systems, like a charge-coupled device (CCD)-based beam profiler, the minimal resolvable spot size is, however, limited by, e.g., the pixel dimension and spacing. Typically, a minimum beam waist of more than about 60  $\mu\text{m}$  is necessary to be well resolved with such beam profiling systems. Yet, for laser micromachining processes, such as laser scribing of thin films for solar cell, display and organic light-emitting diodes (OLED) applications, smaller spot sizes are required [9]. Therefore, common laser beam profilers cannot be used for the characterization of the focused laser beam in the working plane and the beam alignment of the laser system. In addition, due to a potential displacement, the imaging system may not display the laser beam profile at the place where it will machine the material.

We therefore have developed a quality index to evaluate the quality of a Top-Hat beam profiling element and its alignment in the working area based on the ablated geometry of single pulse ablation of thin transparent conductive oxides (TCO). We demonstrate the influence of different alignment parameters of the optical system on the intensity distribution of a Top-Hat laser beam profile and its impacts on the laser ablation geometry. As long as the structure size is much bigger than the thermal diffusion length, the laser ablation of the thin film is mainly driven by the laser fluence [10]. Indium doped tin oxide (ITO) used has a thermal diffusivity of approximately  $2.3 \times 10^6 \text{ m}^2/\text{s}$ , and this leads to a thermal diffusion length of 152 nm for a pulse length of 10 ns.

## 2. Experimental Section

### 2.1. Laser System

We used a 15-W, pulsed, Nd:YVO<sub>4</sub> laser at 1064 nm (EKSPLA Techno35C, Ekspla, Vilnius, Lithuania) with a maximum pulse energy of 750  $\mu\text{J}$ . The pulse duration can be varied between 6 and 20 ns, depending on the pump current and repetition rate (2.5–100 kHz). The laser beam propagates with a TEM<sub>00</sub> profile having a beam quality  $M^2$  of about 1.4. Linear stages in the  $x$ - and  $y$ -direction provide an accuracy of  $\pm 1 \mu\text{m}$  and a travel speed of up to 500 mm/s to move the samples with respect to the laser beam. While using the Top-Hat beam shaper, we adapt a lens system with an effective focal length of  $f = 58 \text{ mm}$ . This lens is mounted on another drive in the  $z$ -direction to adjust the focal position. A combination of a rotatable polarizer and a half wave plate is used for power adjustment.

### 2.2. Material Setup

For our study, we used commercial ITO on a 0.7-mm glass substrate with a film thickness of 110 nm and a high grade of layer homogeneity. A 15-nm SiO<sub>2</sub> layer is deposited between the glass substrate and the TCO to prevent diffusion of metal components from the glass substrate into the above lying TCO. The samples were processed without further pre-treatments of the surfaces. Based on the method proposed by Liu [10], we determine an ablation threshold of 1.05 J/cm<sup>2</sup> at 1064 nm.

### 2.3. Beam Shaping Optics

For our study, we employed two different commercially available Top-Hat focus beam shapers (FBSs), denoted as FBS-1 and FBS-2, from TOPAG [11]. These diffractive elements are able to generate

a Top-Hat beam profile near the Gaussian diffraction limitation [2]. FBS-1 and FBS-2 differ in their spatial modulation, which, in turn, leads to different intensity distributions of the diffracted optical field. In particular, FBS-1 generates a Top-Hat beam profile in the focus with a square type footprint, yet with rounded corners. The conversion efficiency of FBS-1 is about 95%. In contrast, FBS-2 generates a Top-Hat beam profile with the sharp edges of the square-type footprint. However, the conversion efficiency of FBS-2 is reduced to about 90%.

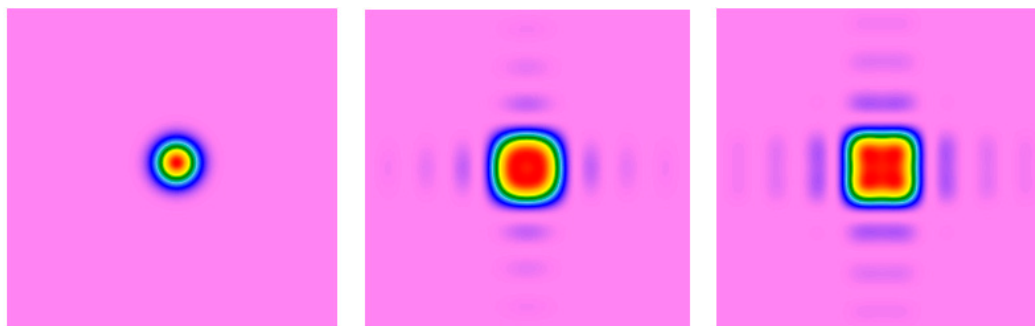
Similar to a Gaussian beam spot, the size of the generated Top-Hat profiles at the 13% level of intensity ( $1/e^2$ ) depends on the wavelength ( $\lambda$ ), the numerical aperture (NA) of the focus lens and the beam quality factor  $M^2$ . The diameter of the Top-Hat profiles at the 13% level can be calculated as follows [4]:

$$\text{Top-Hat size} \approx \frac{\lambda}{\text{NA}} * M^2 \quad (1)$$

The optical setup used in this study generates a Top-Hat beam profile with a diameter in the focus of about  $25 \mu\text{m}$  ( $1/e^2$ ) for both FBS-1 and FBS-2. Common CCD-based beam profilers are not capable of imaging laser spots with these dimensions.

Figure 2 shows a comparison of the simulation results of the intensity distribution in the focal plane using an unshaped Gaussian beam and the beam shapers, FBS-1 and FBS-2. The simulation has been performed using VirtualLab<sup>®</sup> (LightTrans, Jena, Germany).

**Figure 2.** Calculated intensity distribution of the focus beam shaper 1 (FBS-1) (**middle**) and FBS-2 (**right**) Top-Hat beam profile in comparison to a Gaussian beam profile (**left**) [7].



#### 2.4. Method of Evaluation

To demonstrate and evaluate the influence of the optical setup and alignment on the beam shaping result, we vary three different system parameters. Firstly, the distance between the focal lens and the sample, *i.e.*, the position of the working plane is varied. Secondly, the position of a free aperture in front of and behind the beam shaper is changed. Thirdly, the lateral displacement of the diffractive optical element (DOE) is varied. Since the small focus spot size of  $25 \mu\text{m}$  inhibits an evaluation of its intensity distribution by means of a common CCD beam profiler, we developed a method that is based on the ablation geometry of a single laser pulse. For the analysis of the ablation geometry, a laser scanning microscope (Keyence, Osaka, Japan) with a lateral resolution of less than  $50 \text{ nm}$  is used, enabling a precise analysis of the ablated areas. In Figure 3a, an exemplary microscope picture of the generated ablation geometry with a single shaped laser pulse is shown. With the analysis software of the laser scanning microscope, the geometry is gauged as shown in Figure 3b. First the width  $w$  and the length  $l$

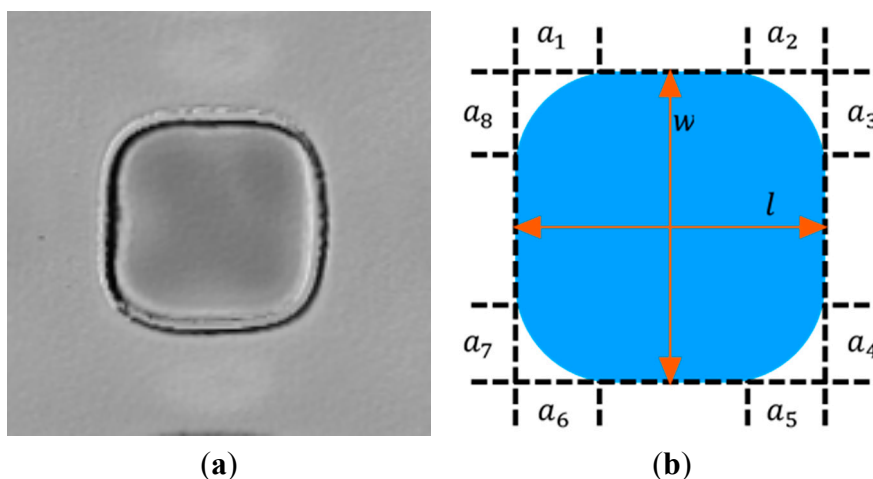
are determined. Subsequently, the size of the corner rounding is analyzed with the parameters  $a_i$  by placing the horizontal and vertical tangents to the boundaries of the ablated geometry. The distance between the intersection points of the tangents and the point where the boundary deviate from the tangents gives 8 separate values for the parameter  $a$ .

To rate the ablation results, we use the measured values and calculate a quality index as follows:

$$\text{quality index } v = \frac{\frac{\sum a_i}{8}}{\frac{l+w}{2}} \tag{2}$$

Please note that the quality index  $v$  can take values between 0 ( $a_i = 0$ ) for an ideal square ablation without corner rounding and 0.5 ( $a_i = w/2$ ) for a complete circle without straight parts.

**Figure 3.** (a) Microscope image of the ablated geometry of a single laser pulse shaped with a Top-Hat beam shaper. (b) Schematic drawing of the evaluation method of the geometry of a shaped single laser pulse.

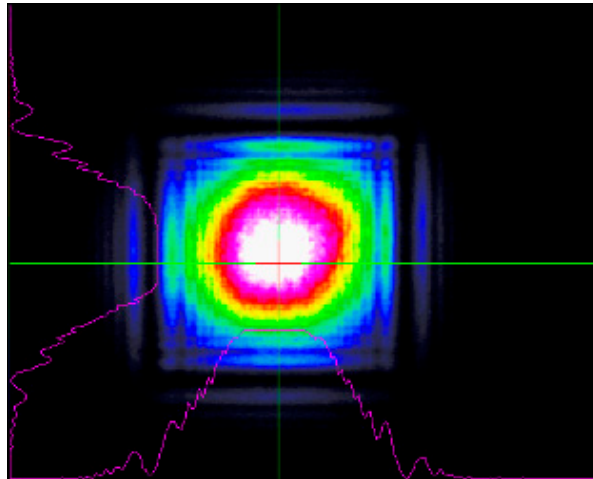


### 2.5. Pre-Alignment

The initial situation of each test requires a defined pre-alignment of the beam shaping optics. Without a focus lens, the laser beam is imaged with a beam profiler (LaserCam HR, Coherent, Santa Clara, CA, USA). The position of the beam shaper can be seen by a dark square (due to the optical mount) in the beam profile (*cf.* Figure 4). This square can be used as an adjustment frame. The beam shaper that is placed in an  $XY$  translation mount is moved to the position where the adjustment frame is centered on the laser beam profile. As is seen in Figure 4, the dark square is centered to the beam, and diffraction effects can be observed. In general, the maximum of the laser intensity should be in the middle of the adjustment frame, and the diffractive patterns should be symmetrical around it. Up to now, no prediction about the quality of the resulting Top-Hat can be made. By introducing the beam profiler into the beam path behind a focus lens, the beam waist decreases with increasing distance between the focus lens and the beam profiler until its dimension is too small for the beam profiler to be resolved (for our equipment, the spatial limit is about 100  $\mu\text{m}$ ). As for FBS, the Top-Hat appears only near the focal position; the CCD-based beam profiler can only be used for pre-alignment, but not for characterization of the beam shaping result in the focus. We therefore used the ablation geometry as measured by the laser scanning microscope to

access information about the alignment and about readjustments of the beam shaper. Several iterations are required to achieve a well-defined ablation geometry.

**Figure 4.** Image of the CCD-based beam profiler showing the pre-alignment step of the laser beam shaper, FBS-1.



### 3. Results and Discussion

#### 3.1. Variation of the Focal Position

When using a diffractive beam shaper, the user has to consider the special propagation properties of the laser beam behind the focus lens. If a Gaussian beam profile is focused, the laser profile remains a Gaussian distribution. A beam that is shaped with FBS alters its beam profile during propagation. The diffraction-limited Top-Hat beam profile only appears at the focal position [4]. Hence, it is necessary to keep the distance between the focus lens and the machined material constant.

To investigate the influence of a shift of the working plane, we ablate thin ITO layers with different focal positions by altering the position of the focus lens with increments of 20  $\mu\text{m}$  with the motorized  $z$ -stage. The generated ablation geometries are analyzed according the quality index  $\nu$ . Figure 5 shows the variation of the quality index *versus* the shift of the working plane for both optical beam profiling elements. For these experiments, an increase of the working plane shift is induced by an increase of the distance between the focus lens and the processed material. Both FBS-1 and FBS-2 qualitatively possess a comparable behavior of the quality index when shifting the working plane. At the focal position, FBS-1 creates a square geometry with the lowest quality index of  $\nu = 0.31$ , whereas FBS-2 leads to a better index of 0.19. The microscope images of these two positions shown in Figure 6a,c confirm this interpretation.

Changing the distance between the focus lens and the material (leaving the focal plane) increases the quality index. As expected, a  $z$ -shift of only +0.1 mm changes the beam profile dramatically, since the diffractive optical elements generate the Top-Hat profile with a rectangular footprint only in the focal point. In the case of FBS-1, for  $z = +0.1$  mm, the ablated geometry becomes circular and the quality index rises up to 0.39 (*cf.* Figure 6b). For FBS-2, the same displacement still leads to a better ablated geometry (a square footprint is still apparent) and an index of 0.28 (Figure 6d). This implies a larger working zone in the  $z$ -direction for FBS-2.

**Figure 5.** The behavior of the quality index for the deviation from the focal position for FBS-1 and FBS-2.

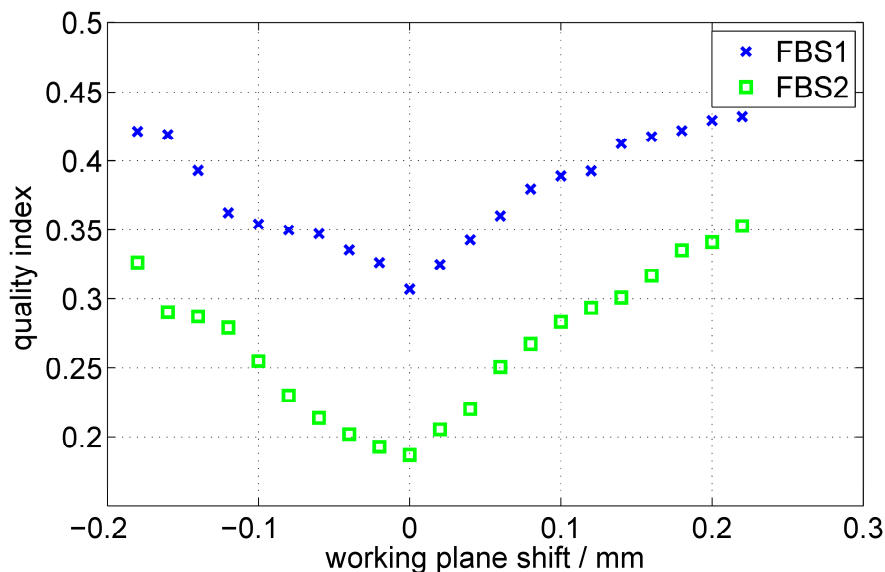
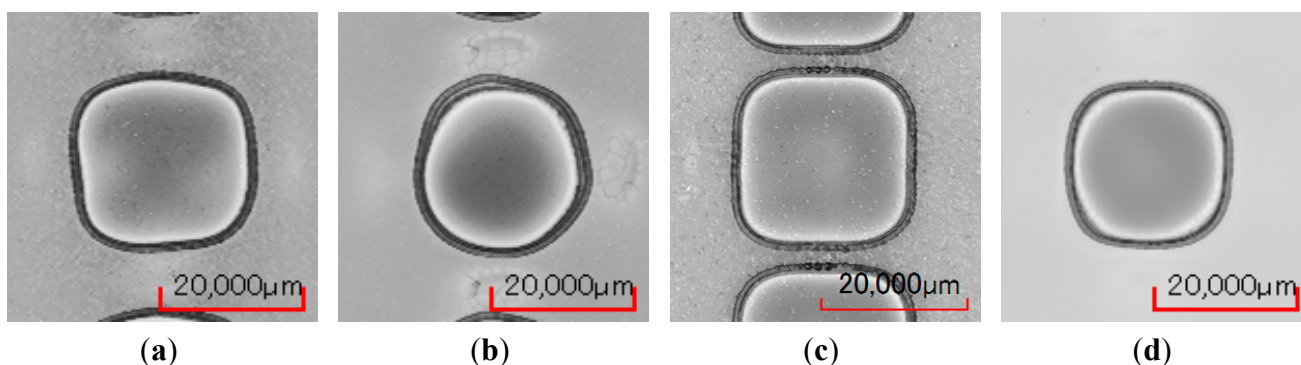


**Figure 6.** Images of the ablated geometry with the beam shapers in the focal position and displaced by 100 μm in the z-direction. (a) FBS-1 z-shift = 0,  $\nu = 0.31$ . (b) FBS-1 z-shift = 0.1 mm,  $\nu = 0.39$ . (c) FBS-2 z-shift = 0,  $\nu = 0.18$ . (d) FBS-2 z-shift = 0.1 mm,  $\nu = 0.28$ .



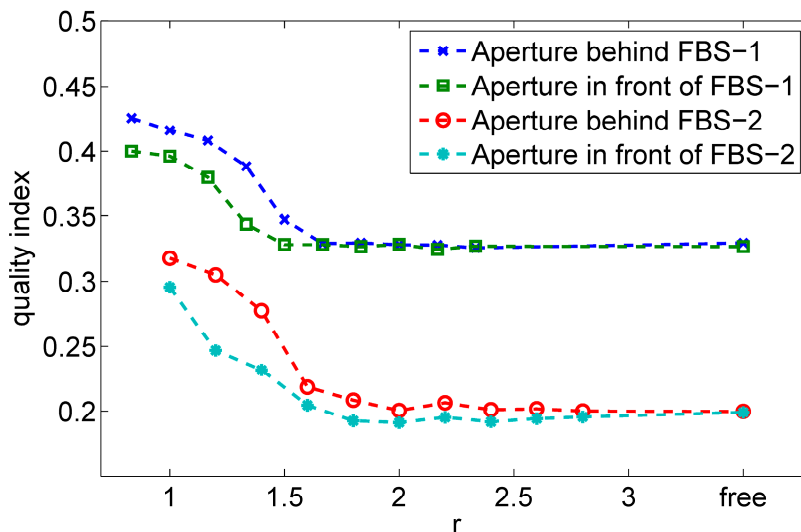
### 3.2. Limitations by a Free Aperture in the Beam Path

The diffractive grating of the beam shaper gives a modulation to the phase of the laser beam that causes the transformation to a Top-Hat beam profile in the focal point of a lens. To achieve a good beam shaping result, the modulation has to take place over a large area of the laser beam profile. For diffractive beam shapers, this area is larger than the beam size, which commonly is defined by an intensity drop to a certain level, e.g.,  $1/e$ ,  $1/e^2$  or full width at half maximum (FWHM). Diffractive beam shapers even use intensity below these levels, *i.e.*, far-off the beam size. Hence, it is necessary to provide a large free aperture in the beam path. We use an adjustable iris diaphragm to limit the free aperture and observe the influence on the quality index for an iris position in front of and behind the beam shapers. The value  $r$  describes the ratio between the size of the free aperture and the beam waist ( $1/e^2$ ) and should help to transfer these results to laser systems with other beam sizes. For FBS-1 and FBS-2, a ratio  $r$  of at least 2.2 is recommended by the supplier, which means the free aperture of the entire laser beam path must be 2.2-times bigger than the beam diameter ( $1/e^2$ ).

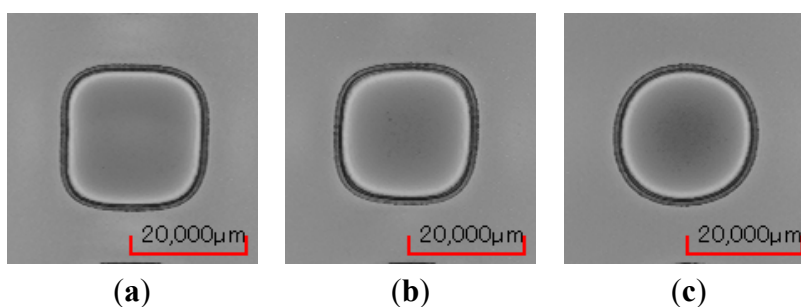
Figure 7 shows the quality index depending on the ratio  $r$  for both FBS-1 and FBS-2. Without the iris diaphragm, the free aperture is limited by standard lens and mirror mounts with a diameter of 1 in. In this case, the initial quality index  $\nu$  for FBS-1 is 0.32 and for FBS-2 0.19, respectively. For FBS-1, the position of the aperture influences the quality index below  $r = 1.6$ , i.e., the free aperture of the entire laser beam path is 1.6-times bigger than the beam diameter. In the case that the aperture is placed behind the beam shaper, the degradation to  $\nu$  is slightly stronger. For  $r$  lower than one, no rectangular beam shape can be observed. The influence of the iris diaphragm on the quality index of ablation geometries with FBS-2 is detectable for a ratio  $r$  below 1.8. Similar to the results of FBS-1, the aperture has also a stronger influence on the quality index if it is placed behind the beam shaper. The stronger degradation of the quality index for experiments with the aperture being placed behind the beam shaper is caused by the fact that in this configuration, the modulated phase information is blocked and cannot be used for beam shaping.

Figure 8 depicts microscope images of ablation geometries using different values of  $r$  with the iris diaphragm placed in front of the beam shaper FBS-2. If the beam path is only limited by the lens and mirror mount with a diameter of 1 in., the corners of the geometry are sharp and the boundaries are almost straight (cf. Figure 8a). The limitation of the beam path to a ratio of  $r = 1.6$  causes stronger rounding of the corners, and the boundaries are slightly curved, as shown in Figure 8b. If the free aperture is smaller than the beam size, the ablation geometry is round, and no rectangular footprint is observable.

**Figure 7.** Influence of the free aperture to the quality index for different positions in the beam path.



**Figure 8.** Behavior of the quality index for deviation from the focal position for FBS-1 and FBS-2. (a) Free aperture/ $\nu = 0.19$ . (b)  $r = 1.6/\nu = 0.22$ . (c)  $r = 0.6/\nu = 0.42$ .



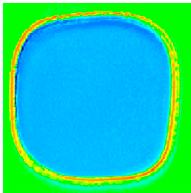
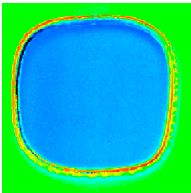
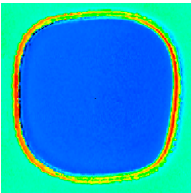
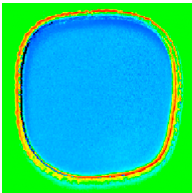
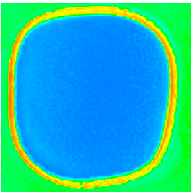
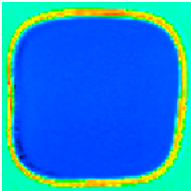
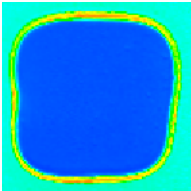
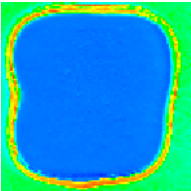
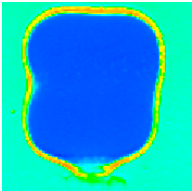
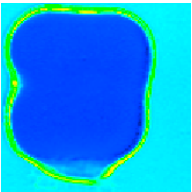
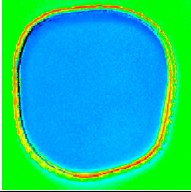
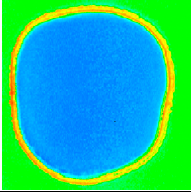
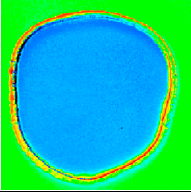
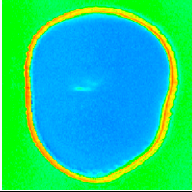
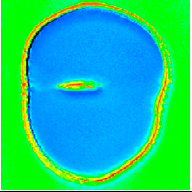
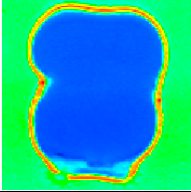
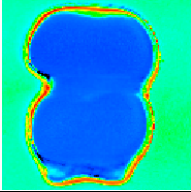
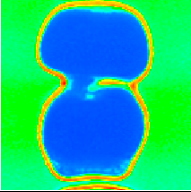
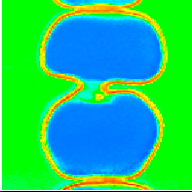
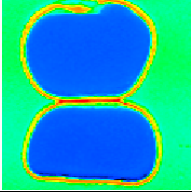


3.3. Lateral Displacement of the Beam Shaping Optical Element

The influence of a lateral displacement of the beam shaping optics is shown in Table 1, highlighting the effect of a lateral misalignment. The lateral shift of the diffractive optical elements has been realized by mounting them on a single-axis micrometer stage. Starting from a well-adjusted beam shaper, we shift the DOE with incremental steps of 250 μm downwards to a total lateral displacement of 2.25 mm and measure the ablation geometry for each step. As large lateral misalignment of the DOE causes a strong contortion of the ablation geometry (*cf.* microscope images in Table 1), the proposed quality index cannot be applied in this section, and the discussion is based qualitatively on the microscope images, only.

Table 1 compares the ablated geometries for different lateral displacements of FBS, *i.e.*, for different beam shaping results. Apparently, FBS-1 shows a high degree of tolerance for misalignment. A lateral shift of up to 750 μm causes no noticeable variation of the ablated geometry. Increasing the displacement up to 2.25 mm stretches the ablation geometry, and it starts to separate. In comparison to FBS-1, the influence of misalignment on the beam shaping result of FBS-2 is noticeably stronger. A lateral displacement of 500 μm stretches the geometry palpable. With increasing misalignment, the ablated area gets a waist and starts to separate. It is worthwhile to mention that these tests only show the influence of a lateral displacement of FBS on the footprint. Additional CCD camera-based investigations of the Top-Hat beam profiles using FBS-1 and FBS-2 with a low NA setup show that upon misalignment, the plateau tilts for lateral misalignment.

**Table 1.** Comparison of the ablated geometry for different lateral displacement values for FBS-1 and FBS-2.

Lateral Displacement	0 μm	250 μm	500 μm	750 μm	1 mm
FBS-1					
FBS-2					
Lateral Displacement	1.25 mm	1.50 mm	1.75 mm	2 mm	2.25 mm
FBS-1					
FBS-2					

#### 4. Conclusions

Based on an experimental study of thin film laser ablation using laser Top-Hat beam profiling optics, we have proposed a method to evaluate the beam shaping result with the help of the ablation geometry and an objective assessment of the Top-Hat using a quality index that describes the geometry of single pulse ablation. Secondly, we have demonstrated the critical influence of optical alignment on the laser ablation result. In particular, the impact of the focal position, a free aperture in the beam path and the lateral displacement of the beam shaper are highlighted based on the quality index and microscope images of the laser ablation. The results provide valuable support for industrial users of beam shaping optics to appraise the root causes of defective micro-material processing results using diffractive beam shaping optics.

#### Acknowledgments

The authors thank Erwin Jäger and Christian Bischoff from TOPAG for allocation of the beam shapers, FBS-1 and FBS-2, and their valuable support.

#### Author Contributions

Stefan Rung and Johannes Barth did the experiments and develop the evaluation method. Prof. Dr. Ralf Hellmann supervise the work. Stefan Rung and Prof. Dr. Ralf Hellmann wrote and revised the manuscript.

#### Conflicts of Interest

The authors declare no conflict of interest.

#### References

1. Baird, B.; Gerke, T.; Wieland, K.; Paudel, N. P2 and P3 Spatially Shaped Laser Scribing of CdTe and a-Si Thin Film Solar Cells Using a 532 nm Picosecond MOFPA. In Proceedings of 26th European Photovoltaic Solar Energy Conference and Exhibition, Hamburg, Germany, 5–8 September 2011; pp. 2471–2474.
2. Raciukaitis, G.; Stankevicius, E.; Gecys, P.; Gedvilas, M.; Bischoff, C.; Jäger, E.; Umhofer, U.; Völklein, F. Laser processing by using diffractive optical laser beam shaping technique. *J. Laser Micro/Nanoeng.* **2011**, *6*, 37–43.
3. Steiger, E.; Scharnagl, M.; Kemnitzer, M.; Laskin, A. Optimization of the Structuring Processes of CI(G)S Thin-Film Solar Cells with an Ultrafast Picosecond Laser and a Special Beam Shaping Optics. In Proceedings of 28th International Congress on Applications of Lasers & Electro-Optics (ICALEO), Orlando, FL, USA, 2–5 November 2009.
4. Rung, S.; Rexhepi, M.; Bischoff, C.; Hellmann, R. Laserscribing of thin films using Top-Hat laser beam profiles. *J. Laser Micro/Nanoeng.* **2013**, *8*, 309–314.

5. Hauschild, D.; Homburg, O.; Mitra, T.; Ivanenko, M.; Jarczyński, M.; Meinschien, J.; Bayer, A.; Lissotschenko, V. Optimizing Laser Beam Profiles Using Micro-Lens Arrays for Efficient Material Processing: Applications to Solar Cells. In Proceedings of SPIE 7202 Laser-Based Micro- and Nanopackaging and Assembly III, San Jose, CA, USA, 28–29 January 2009; doi: 10.1117/12.809270.
6. Bovatsek, J.; Patel, R.S. High-Power ns-Pulsed Q-switched Laser Technology with Flattop Beam-Shaping Technique for Efficient Industrial Laser Processing. In Proceedings of 28th International Congress on Applications of Lasers & Electro-Optics (ICALEO), Orlando, FL, USA, 29 October–1 November 2007.
7. Rung, S.; Bischoff, C.; Jäger, E.; Umhofer, U.; Hellmann, R. Laser Thin Film Ablation with Multiple Beams and Tailored Beam Profiles. In Proceedings of SPIE 8967 Laser Applications in Microelectronic and Optoelectronic Manufacturing (LAMOM) XIX, San Francisco, CA, USA, 3–6 February 2014; doi:10.1117/12.2038572.
8. Eidelloth, S.; Neubert, T.; Brendemühl, T.; Hermann, S.; Giesel, P.; Brendel, R. High Speed Laser Structuring of Crystalline Silicon Solar Cells. In Proceedings of 34th IEEE Photovoltaic Specialists Conference (PVSC), Philadelphia, PA, USA, 7–12 June 2009; pp. 002389–002394.
9. Tsai, C.Y.; Tsai, C.Y. Development of amorphous/microcrystalline silicon tandem thin-film solar modules with low output voltage, high energy yield, low light-induced degradation, and high damp-heat reliability. *J. Nanomater.* **2014**, *2014*, 861741, doi:10.1155/2014/861741.
10. Liu, J.M. Simple technique for measurements of pulsed Gaussian-beam spot sizes, *Opt. Lett.* **1982**, *7*, 196–198.
11. TOPAG. Available online: <http://www.topag.de> (accessed on 1 October 2014).

© 2014 by the authors; licensee MDPI, Basel, Switzerland. This article is an open access article distributed under the terms and conditions of the Creative Commons Attribution license (<http://creativecommons.org/licenses/by/4.0/>).